

# Search for the minimal universal extra dimension model at the LHC with $\sqrt{s}=7$ TeV

Biplob Bhattacharjee<sup>a</sup> and Kirtiman Ghosh<sup>b</sup>

<sup>a</sup>Department of Theoretical Physics, Tata Institute of Fundamental Research,  
1, Homi Bhabha Road, Mumbai 400 005, India.  
E-mail: biplob@theory.tifr.res.in,

<sup>b</sup>Harish Chanda Research Institute, Chhatnag Road,  
Jhansi, Allahabad 211019, India  
E-mail: kirtiman@hri.res.in.

## Abstract

Universal Extra Dimension (UED) model is one of the popular extension of the Standard Model (SM) which offers interesting phenomenology. In the minimal UED (mUED) model, Kaluza-Klein (KK) parity conservation ensures that  $n = 1$  KK states can only be pair produced at colliders and the lightest KK particle is stable. In most of the parameter space, first KK excitation of SM hypercharge gauge boson is the lightest one and it can be a viable dark matter candidate. Thus, the decay of  $n = 1$  KK particles will always involve missing transverse energy ( $\cancel{E}_T$ ) as well as leptons and jets. The production cross sections of  $n = 1$  KK particles are large and such particles may be observed at the Large Hadron Collider (LHC). We explore the mUED discovery potential of the LHC with  $\sqrt{s} = 7$  TeV in the multileptonic final states. Since in the early LHC run, precise determination of  $\cancel{E}_T$  may not be possible, we examine the LHC reach with and without using  $\cancel{E}_T$  information. We observe that  $\cancel{E}_T$  cut will not improve mUED discovery reach significantly. We have found that opposite sign di-lepton channel is the most promising discovery mode and with first  $fb^{-1}$  of collected luminosity, LHC will be able to discover the strongly interacting  $n = 1$  KK particles with masses upto  $800 \sim 900$  GeV.

PACS numbers: 13.85.Qk, 12.60.-i, 14.80.Rt

Keywords: Universal Extra Dimension, LHC, Multilepton search

# I Introduction

The Universal Extra Dimension (UED) model, proposed by Appelquist, Cheng and Dobrescu [1], appears to be one of the popular scenario beyond the Standard Model (SM). This model assumes that all particles can propagate in the flat extra dimensions and in its minimal version (mUED) [2, 3], there is only one extra dimension  $y$  compactified on a circle of radius  $R$  ( $S_1$  symmetry). An additional  $Z_2$  symmetry, which identifies  $y$  to  $-y$  is required to get zero mode chiral fermions at low energy. The  $Z_2$  symmetry breaks the translational invariance along the 5th dimension and generates two fixed points at  $y = 0$  and  $y = \pi R$ . The size of the extra dimension is taken to be small enough so that one can dimensionally reduce the theory and construct the effective 4D Lagrangian. The low energy effective Lagrangian contains infinite number of Kaluza-Klein (KK) excitations (identified by an integer number  $n$ , called the KK number) for all the fields which are present in the higher dimensional Lagrangian. The zero modes of the KK towers are generally identified with the Standard Model particles.

On the other hand, there is a particular variant of the UED model, called two Universal Extra Dimension (2UED) model [4], where all the SM fields propagate in  $(5 + 1)$  dimensional space time. 2UED model has some additional attractive features. As an example, 2UED model can naturally explain the long life time of proton [5] and more interestingly it predicts that the number of fermion generations should be an integral multiple of three [6]. The phenomenology of KK-excitations of 2UED model has been studied in great detail in recent times which covers its implications at colliders [7], in various low-energy observables [8] and dark matter/cosmology [9]. However, in this article, we will only concentrate on the phenomenology of mUED model at the Large Hadron Collider (LHC).

One of the interesting feature of the mUED model is the conservation of KK number. Since all particles can propagate in the extra dimension, the momentum along the extra dimension is conserved and it is also quantized because of the compactification of the extra dimension  $y$ . The five dimensional momentum conservation is translated into the conservation of KK number in the four dimensions. However, the presence of two fixed points break the translational symmetry and KK number is not a good quantum number. In principle, there may exist some operators located at these fixed points and one can expect mixing among different KK states. However, if the localized operators are symmetric under the exchange<sup>1</sup> of the fixed points, the conservation of KK number breaks down to the conservation of KK parity defined as  $(-1)^n$ , where  $n$  is the KK number. The conservation of KK parity ensures that  $n = 1$  particles are always produced in pairs and the lightest  $n = 1$  particle (LKP) must be stable. It also forbids tree level mUED contribution to any SM process. The situation is analogous to the  $R$  parity conserving supersymmetric models [10]. The tree level mUED spectrum is extremely degenerate and first excitation of any massless SM particle can be the LKP (say KK excitation of gluon, photon, neutrino i.e.,  $g_1$ ,  $\gamma_1$ ,  $\nu_1$  etc.). The radiative corrections [2, 11, 12] play very important role in determining the mUED mass spectrum. The correction terms can be finite (bulk correction) or it may depends on the cut-off of the model  $\Lambda$  (boundary correction). The cut-off dependence comes from the fact that mUED is a higher dimensional model and thus,

---

<sup>1</sup>This is another  $Z_2$  symmetry, but not the  $Z_2$  of  $y \leftrightarrow -y$ .

it is nonrenormalizable. This model should be treated in the spirit of an effective theory valid upto a scale  $\Lambda > R^{-1}$ . It is shown in the literature [2] that radiative correction partially removes the degeneracy in the spectrum and in most of the parameter space  $n = 1$  excitation of hypercharge gauge boson  $B$  called  $\gamma_1$ <sup>2</sup>, is the LKP. The  $\gamma_1$  can produce the right amount of cosmological relic density (consistent with the WMAP data) and turns out to be a good dark matter candidate [13]. The mass of LKP is approximately  $R^{-1}$  and hence, the overclosure of the universe puts an upper bound on  $R^{-1} < 1400$  GeV. The lower limit of  $R^{-1}$  comes from the low energy observables and direct search of new particles at the Tevatron. Constraints on  $R^{-1}$  from  $g - 2$  of the muon [14], flavour changing neutral currents [15, 16, 17],  $Z \rightarrow b\bar{b}$  decay [18], the  $\rho$  parameter [1, 19], other electroweak precision tests [20], hadron collider studies [21, 22] imply that  $R^{-1} \gtrsim 300$  GeV. A recent inclusive  $\bar{B} \rightarrow X_s \gamma$  analysis sets a stronger constraint  $R^{-1} \gtrsim 600$  GeV at 95% CL [23], although it still keeps open a lower value of  $R^{-1} \sim 400$  GeV at 99% CL. The lower and upper bounds indicate that atleast pair production of  $n = 1$  excited states are possible at the LHC. The masses of KK particles are dependent on  $\Lambda$  which has no determined value. One loop corrected  $SU(3)$ ,  $SU(2)$  and  $U(1)$  gauge couplings show power law running in the mUED model and almost meet at the scale  $\Lambda = 20 R^{-1}$  [24, 25]. Thus, one can take  $\Lambda = 20R^{-1}$  as the cut-off of the model and expect the presence of some new physics above that energy scale. If we neglect such type of unification, we can extend the value of the cut-off, but at the scale around  $40 R^{-1}$ ,  $U(1)$  coupling becomes nonperturbative. Thus, the cut-off  $\Lambda R$  of the mUED model should not be taken above 40 and one should use the value of  $\Lambda R$  between 10 to 40.

The collider phenomenology of mUED model is similar to the  $R$  parity conserving supersymmetry and it has been investigated in Ref. [26], though not with the same level of detail and sophistication as the corresponding signals from supersymmetry [27, 28]. The crucial feature of these studies is the existence of the stable LKP (KK parity conservation) and hence, the missing energy and missing transverse momentum signal at the colliders. The current bounds allow KK states to be as light as a few hundreds of GeV. Such light  $n = 1$  particles can be pair produced at the LHC and they cascade down to  $\gamma_1$  which escapes the detector. Like  $R_p$  conserving SUSY, the characteristic signature of mUED is leptons plus jets accompanied by missing energy. The SM particles arising from the decay of KK particles are usually soft. It is due to the partial degeneracy in the mUED spectrum<sup>3</sup>. The model predictions depend only on the two parameters  $R^{-1}$  and  $\Lambda$ .

One of the cleanest signal for new physics search is the multiple leptons in the final state. Leptonic signals at the LHC with missing energy have been studied in the literature particularly in the context of SUSY searches. In the present work, we also consider leptonic final states and systematically study the capability of LHC with  $\sqrt{s} = 7$  TeV in the discovery of mUED. We

---

<sup>2</sup>Actually in the presence of radiative correction, the KK Weinberg angle is small so that  $B_1 \approx \gamma_1$  and  $W_1^3 \approx Z_1$ .

<sup>3</sup>This feature uncommon in most of the supersymmetric models and one can use this to discriminate mUED from different supersymmetric scenarios [29].

consider two<sup>4</sup> to four leptons accompanied by jets and missing transverse energy in the final states. There are two motivations for our present study. First, most of the phenomenological study on mUED was carried out using parton level monte carlo simulations and a more detailed analysis is required at this stage. The other reason is that people have studied mUED model by assuming centre of mass energy of LHC to be equal to 14 TeV but, LHC has started its operation with reduced CM energy of 7 TeV and it will collect data upto  $1\text{fb}^{-1}$ . It is therefore, useful to recalculate the mUED discovery reach of LHC with CM energy 7 TeV. The rest of the paper is arranged as follows. In the next section, we shall discuss the production of multileptonic final states in mUED model and comment on possible SM backgrounds. In section III, we shall define the final states, event selection criteria and explore the discovery reach of the LHC. Finally, section IV summarizes our main results and addresses the possible issues of this work.

## II Leptonic signals of mUED model

Leptonic final states are always represented as the most powerful discovery channels at the hadron collider. The detectors of LHC have the ability to identify the leptons very efficiently within a very wide energy range. In mUED model, leptonic branching ratios are always favorable and multilepton signals can become competitive to the SM backgrounds.

At the LHC, the dominant production processes of mUED are the pair production of  $n = 1$  KK quarks and KK gluons. Typical mUED spectrum shows that the colored KK states are heavier than the electroweak KK particles and  $n = 1$  gluon  $g_1$  is the heaviest. It can decay to both  $n = 1$  singlet ( $q_1$ ) and doublet ( $Q_1$ ) quarks with almost same branching ratios, although, there is a slight kinematic preference to the singlet channel. The singlet quark can decay only to  $\gamma_1$  and SM quark. On the other hand, doublet quarks decay mostly to  $W_1$  or  $Z_1$  (which are KK excitation of electroweak gauge boson  $W$  and  $Z$ ). Hadronic decay modes of  $W_1$  and  $Z_1$  are closed kinematically and these can decay universally to all  $n = 1$  doublet lepton flavours ( $L_1$  or  $\nu_1$ ).  $W_1$  decays to  $L_1^\pm \nu_L$  or  $L^\pm \nu_1$  with equal branching ratios. Similarly,  $Z_1$  can decay only to  $L_1 l$  or  $\nu_1 \nu$ . The KK leptons finally decay to  $\gamma_1$  and a ordinary (SM) lepton. The  $\gamma_1$  will escape the detector because it has no strong and electromagnetic interactions. Thus, the resulting signature would then be  $n$  jets +  $m$  leptons + missing  $E_T$ . The pair production of  $n = 1$  singlet quarks ( $q_1$ ) lead to 2 jets plus missing energy signature. Multijet with missing energy signal has become a canonical signature for SUSY search. To reduce the SM background contributions, all such analysis demand that the missing transverse energy must be greater than 200 GeV. In the next section, we shall show that the  $\cancel{E}_T$  distribution of mUED models is softer and thus, such type of cut will kill the SM backgrounds as well as mUED signal. Therefore, the more interesting processes that we can consider are  $g_1 g_1$ ,  $g_1 Q_1$  or  $Q_1 Q_1$ , where  $Q_1$  is the  $n = 1$  doublet KK quarks. In this case, the leptons are produced from the cascade decay of  $W_1$  and  $Z_1$ . The number of lepton may vary from 1 to 4. At this point, let us comment on third generation KK states. The singlet and doublet KK states are not exactly the mass eigenstates.

---

<sup>4</sup>We do not consider single lepton channel here. This is because, SM background coming from the  $W$  production is huge and can not be eliminated by choosing proper cuts.

In the doublet-singlet basis, mass matrix is non-diagonal, and the off-diagonal elements are the zeroth level mass  $M_0$ . We can neglect the SM masses of the quarks and leptons with respect to  $R^{-1}$  except for the third generation quarks. After diagonalisation and a chiral rotation, one gets the proper mass eigenstates called  $\tilde{q}_1$  and  $\tilde{q}_2$ . In case of KK top quarks, the doublet singlet mixing is most prominent.  $\tilde{t}_1$  can decay dominantly to charged KK Higgs, and  $\tilde{t}_2$  can decay to  $W_1$  or  $Z_1$ . Generally the KK top quarks are taken separately in the analysis and it is not included in our results. The decay of doublet b KK quark to SM top and  $W_1$  is not allowed kinematically and its main decay mode is SM  $b$  quark with  $n = 1$  Z boson.

At the LHC, one can also have associated production of a  $n = 1$  KK electroweak gauge boson together with a  $n = 1$  KK quark. Such processes also contribute to the multileptonic final states with low jet multiplicity, but the cross sections are much lower than the strong cross sections. As an example,  $Q_1 W_1$  production cross section is around 5 pb for  $R^{-1}=300$  GeV and  $\Lambda R=20$  at LHC with centre of mass energy 14 TeV, whereas strong KK pair production is around 2000 pb. Similarly, the production and decays of the  $n = 2$  particles result in final states with leptons. Inclusion of all such processes will definitely increase the mUED discovery reach at the LHC, but our analysis is restricted to the pair production of strongly interacting KK particles only.

The KK quarks and gluons carry colours and it is needless to mention that their production cross sections are high at the LHC. The tree level KK number conserving couplings of KK quarks and gluons are similar to SM couplings and there is no  $\Lambda$  or  $R$  dependence in their couplings. However, the masses of the KK states are logarithmically cut-off dependent and thus, the KK production cross sections depend mildly on the cut-off. Here we fix the value of  $\Lambda R$  equals to 20 and plot the the leading order pair production cross sections of coloured  $n = 1$  KK states as a function of  $R^{-1}$  at the LHC with  $\sqrt{s}=7$  TeV. For completeness, we also plot the same for LHC with  $\sqrt{s}=14$  TeV. We use CTEQ5L parton distribution function and the scale of the strong coupling constant is taken to be equal to the parton level center of mass energy. Here we sum over the final state quark flavors and include charge-conjugated contributions.

From Fig. 1, we see that at the 7 TeV LHC, if  $R^{-1}$  is less than 600 GeV,  $q_1/Q_1 g_1$  cross section is dominant and the cross sections fall off rapidly with  $R^{-1}$ . The cascade decay of  $Q_1 g_1$  events generally produce 3 jets, leptons and missing energy. At the LHC with  $\sqrt{s}=7$  TeV, the total mUED pair production cross section is about 100 pb for  $R^{-1}=300$  GeV and it is around 1pb for  $R^{-1}=800$  GeV corresponding to  $10^5$  to  $10^3$  events with  $1fb^{-1}$  of luminosity. From this naive result, we may say that even with small amount of data, we can get some hints of KK particles. The reach of the 14 TeV LHC is much higher and a run with moderate luminosity has the capability to probe the entire dark matter allowed region of mUED parameter space. Again in case of 14 TeV LHC,  $Q_1 g_1$  rate is the highest upto  $R^{-1}=1200$  GeV, above which  $n = 1$  quark pair production is comparable. It is to be noted that we have used the leading order cross sections from PYTHIA [30], but the higher order correction to the mUED processes should be significant.

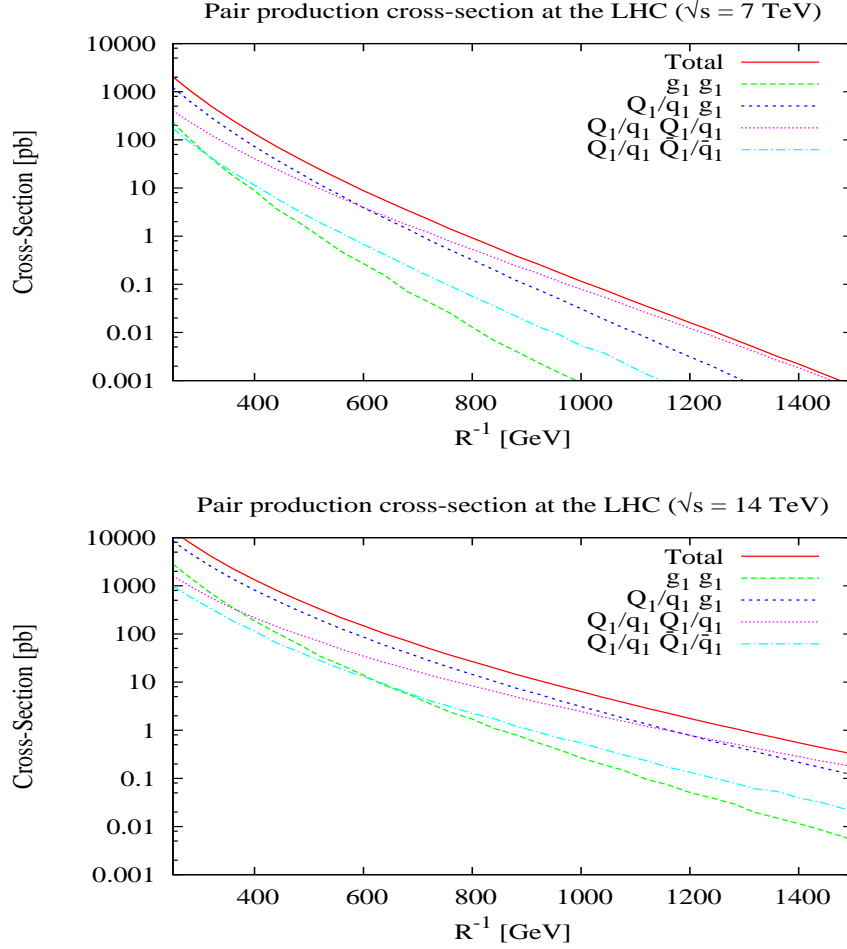


Figure 1: Cross sections for the pair production of  $n=1$  quarks and gluons at the LHC as a function of  $R^{-1}$ .  $\Lambda R$  is kept fixed at 20. The top figure is for center of mass energy 7 TeV whereas the bottom is for center of mass energy 14 TeV.

We are now in a position to specify the final states used in our analysis. In this part, we shall briefly describe how one can get di-leptons, tri-leptons and four leptons associated with jets and missing transverse momentum in the mUED model. We shall also comment on the possible SM backgrounds. In the SM, leptonic final states arise from the decay of  $W/Z$  boson, top quark or from the semileptonic decay of heavy flavours. The Standard Model background processes most relevant to mUED searches are  $t\bar{t}$ ,  $W$  plus jets,  $Z$  plus jets, diboson production etc. A good understanding of such processes are essential and precise predictions provide a high sensitivity to searches for new phenomena producing multi-leptonic final states.

**2l final state:** We look for an excess over the SM background in a final state that contains exactly equal to two leptons ( $e$  or  $\mu$ ) plus jets and significant amount of missing energy. The leptons can have same or opposite charges. In the mUED model, the opposite sign di-leptons

can be produced from the production of opposite sign doublet quarks (like  $U_1 \bar{U}_1$  production) and its decay through  $W_1^\pm$ . The each  $W_1$  can produce one lepton and these two leptons have opposite charges. The production of  $g_1 Q_1$  and  $g_1 g_1$  followed by the 2 body decay of KK gluon to doublet KK quarks can also produce two opposite sign doublet quarks. KK  $Z$  boson is another source of di-leptons. The same sign di-lepton production mechanism is similar to the opposite sign case. In this case, two same sign doublet quark is needed which can be produced directly or from the  $g_1 Q_1$  and  $g_1 g_1$  processes. The same sign doublet quark pair production via the exchange of KK gauge bosons (mainly  $g_1$ ) is the most significant production mechanism. One can easily estimate the number of di-leptons in the final state from the knowledge of cross sections, because the branchings are quite insensitive to the model parameters of the model. The OSD final state has a higher rate than the SSD final state. The advantage of SSD over OSD signal is that it is almost background free. The most significant SM background of same sign di-lepton is coming from  $t\bar{t}$  production followed by the semileptonic decay of  $t\bar{t}$  pairs. Here the second lepton originates from the semileptonic  $b$  decay. The  $b\bar{b}$  production can also be a dangerous background where the both leptons may come from  $b$  decay. The leptons from the decay of  $b$  quarks are generally soft and non isolated from the associated jets. Therefore, by requiring high  $p_T$  leptons and tight isolation criteria one can suppress such background. In addition, diboson production also contributes to the background. In real experiment, charge mismeasurement of lepton is also possible. This can turn an opposite-sign pair into a like-sign pair. Estimate of the sign misidentification rate is necessary and it should be included in the study. But, we have not done any detector simulation and hence, charge misidentification is neglected. In case of opposite sign di-lepton final state,  $Z$  boson,  $t\bar{t}$  and diboson production are dominant backgrounds. By putting invariant mass cut on the di-leptons,  $Z$  boson background can be reduced, but  $t\bar{t}$  background is irreducible. In mUED model, the leptons and jets are generally soft and the missing transverse energy distribution is also soft. So, it is not possible to reduce SM  $t\bar{t}$  background by applying hard cuts on the final state leptons, jets or missing  $E_T$ .

**3l final state** Next we consider tri-leptonic final state. Isolated tri-lepton signal comes from the cascade production of  $W_1 Z_1$  gauge boson pairs and their leptonic decays. In SUSY, first chargino and second neutralino are lighter than the gluino and squarks, and typically masses of these particles lie in the range 200-300 GeV. Therefore, chargino neutralino production rate is expected to be high at the LHC. The production of neutralino chargino pair leads to the hadronically quiet tri-lepton signal which is treated as the golden discovery channel for SUSY. In case of mUED, the masses of the  $W_1$  or  $Z_1$  are  $\sim R^{-1}$ , therefore,  $W_1 Z_1$  direct pair production cross section is much smaller than the SUSY chargino neutralino production rate. For this reason, one has to consider the cascade decay of KK coloured states to electroweak gauge bosons. Thus, in case of mUED, tri-lepton signal is usually associated with jets. The of jets coming from the decay of KK quarks and gluons generally soft and a small fraction of the events may be hadronically quiet. Several SM processes can mimic the tri-lepton signature. The main backgrounds to the tri-leptons are from  $t\bar{t}$ ,  $t\bar{t}Z$ ,  $t\bar{t}W$ ,  $ZZ$ ,  $WZ$  etc. The backgrounds containing an real  $Z$ -boson can be rejected by choosing the invariant mass of the same flavour oppositely charged lepton to be less than 80 GeV or more than 100 GeV.

**4/ final state** The four lepton signals originates from the direct or cascade production of a pair of  $Z_1$  boson via the decay mode  $Z_1 \rightarrow l_1 l \rightarrow ll\gamma_1$ , although, the direct production rate is smaller than the cascade production rate. The dominant SM backgrounds to the four lepton signal are continuum production of  $Z^*/\gamma^* Z^*/\gamma^*$ , real ZZ production, heavy flavour production,  $b\bar{b}b\bar{b}$ ,  $t\bar{t}b\bar{b}$  and Z production associated with heavy flavour. The cross sections of such processes are generally small and by using proper cuts like lepton isolation, Z veto, the backgrounds can be reduced significantly. The four lepton signal is the smallest among all of the multilepton states in mUED. It should be remembered that leptons coming from the decay of KK electroweak gauge bosons or KK leptons are generally soft. In some cases, it is possible to miss one or two of the four leptons.

## III Analysis

We shall now describe our numerical analysis methods and results. In our scan, we vary radius of compactification ( $R^{-1}$ ) from 250 GeV to 1000 GeV although the upper limit, consistent with the mUED dark matter bound, is around 1400 GeV. The reason behind it is that we are trying to discover mUED signals at the LHC in the early stages of its operation. The luminosity is expected to be small and thus, only signals with large cross section will be observed. The total mUED cross section is around 100 fb for  $R^{-1} \sim 1000$  GeV. We shall also study the discovery reach as a function of cut-off  $\Lambda$  of the model. Since the value of the cut-off determines the overall splitting among KK particles, we expect that mUED search sensitivity will also depend on this parameter. Given the value of  $R^{-1}$  and the cut-off one can easily calculate the one loop masses of the KK particles using the formulae given in the Ref. [2].

### III.1 Object Selection

In our analysis, we have introduce a set of basic selection criteria to identify electrons, muons, jets and missing transverse energy. The object selection is described in brief in the following.

#### III.1.1 Electrons/Muons

The following criteria are used to select a electron/muon candidate:

- The transverse momentum  $p_T$  of the electron or muon must be greater than 10 GeV and pseudorapidity  $|\eta| \leq 2.5$ .
- We require that the leptons be isolated from hadronic activity in the detector. To select isolated electrons/muons, we demand that the sum of calorimeter energy within a distance



$\Delta R = 0.2$  (where  $\Delta R = \sqrt{\Delta\eta^2 + \Delta\phi^2}$ ) around the electron/muon candidate must be less than 10 GeV.

- We also use lepton jet isolation cut. We remove electrons that are found within a distance  $0.2 \leq \Delta R \leq 0.4$  from the jet. We also remove all muon candidates fall within a distance  $\Delta R = 0.4$  from a jet.

### III.1.2 Jets

Jets are reconstructed with the help of the inbuilt PYTHIA cluster routine PYCELL. PYCELL uses a fixed-size cone algorithm for clustering. We have use a cone radius of  $\Delta R = 0.4$ . The following selection criteria are introduced to select a jet candidate.

- The minimum  $p_T$  of a jet is taken to be 20 GeV and we also demand  $|\eta_j| < 2.5$ .
- Since electrons are likely to be reconstructed also as jets, we remove any jet candidate that falls within a distance  $\Delta R = 0.2$  of a electron candidate.

### III.1.3 Missing transverse energy, $\cancel{E}_T$

Neutrinos and the  $\gamma_1$  escape the detector, leading to significant missing transverse energy. The missing transverse energy in an event is calculated using calorimeter cell energy and the momentum of the reconstructed muons in the muon spectrometer. In our analysis, we have used the very simplified following definition for the missing transverse energy:

$$\cancel{E}_T = \sqrt{(\sum p_x)^2 + (\sum p_y)^2}, \quad (1)$$

where, the sum goes over all the isolated electrons, muons, the jets.

## III.2 Signal distributions

In this subsection, we briefly study various distributions like missing transverse energy ( $\cancel{E}_T$ ), hardness of the jets and leptons, jet multiplicity etc. of the mUED model. We first examine missing transverse energy distribution. In the generic SUSY search, one of the most powerful discriminator of the signal from the SM backgrounds is the missing transverse energy. We have seen in the previous section that mUED production cross section at the LHC is dominated by the  $n = 1$  KK quarks and gluons which decay through a chain to the lightest KK particle  $\gamma_1$ . In the KK parity conserving model,  $\gamma_1$  escapes the detector and gives rise to missing transverse energy. Thus  $n = 1$  particle production is always associated with  $\cancel{E}_T$ . However, since we are considering nearly degenerate KK spectrum, the final state particles will be soft and thus, it is expected that the  $\cancel{E}_T$  distribution will be softer than a typical SUSY  $\cancel{E}_T$  distribution.

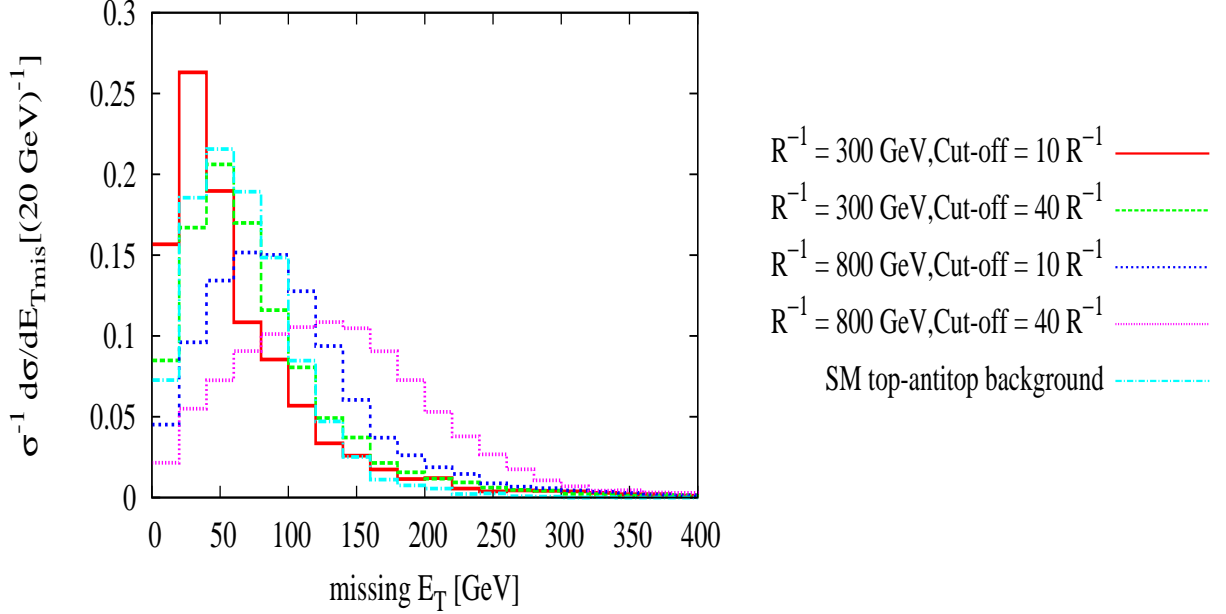


Figure 2: Normalized missing  $E_T$  distribution of the events with no. of leptons  $\geq 2$  for four signal points:  $(R^{-1}, \Lambda R) \equiv (300, 10)$ ,  $(300, 40)$ ,  $(800, 10)$  and  $(800, 40)$  GeV and SM  $t\bar{t}$  background.

In Fig.2, we plot normalized  $E_T$  distributions for different values of  $R^{-1}$  and  $\Lambda R$ . We have presented the distributions for four different signal points, namely,  $(R^{-1}, \Lambda R^{-1}) \equiv (300, 10)$ ,  $(800, 10)$ ,  $(300, 40)$  and  $(800, 40)$  GeV. We also show  $E_T$  distribution of SM  $t\bar{t}$  production. Fig. 2 shows that, for higher value of  $R^{-1}$  and  $\Lambda R$ , missing  $E_T$  increases due to the partial removal of the degeneracy of the mUED mass spectrum. For  $R^{-1}=300$  GeV and  $\Lambda R=40$ , the  $E_T$  peaks at around 50 GeV, and it peaks at 130 GeV for  $R^{-1}=800$  GeV and  $\Lambda R=40$ . In the Standard Model, only sources of missing transverse energy are standard model neutrinos. Thus, the major SM backgrounds which offer missing transverse energy are  $W$ ,  $Z$  and  $t$  production. Various other effects like mismeasurement of jet energy, cracks in the detector can also generate sizeable amount of missing transverse energy. In order to estimate the missing energy originated from such effects, one has to understand the detector properly and it will take a good amount of time for detector calibration. In the early stage of LHC run, missing energy may not be measured accurately. It is therefore reasonable to study the reach of LHC without using  $E_T$  information. The missing  $E_T$  distribution of mUED is not much different from SM and thus hard cut on the missing  $E_T$  will remove majority of the signal events. In this paper, we have demonstrated two different possibilities, e.g., (a). reach of LHC with soft  $E_T$  cut, (b). LHC reach without using missing  $E_T$  cut on the signals as well as backgrounds. For better signal significance, one can optimize the cut on the missing  $E_T$  and hardness of the leptons and jets depending on the masses of the KK particles however, no such

attempt is made in our analysis.

We next show the  $p_T$  distributions of leptons and jets coming from the decay of KK particles. Since we are concentrating only on 2, 3 and 4-lepton events, we have used all the events with number of lepton  $\geq 2$  to numerically evaluate those distributions. In the Fig. 3, we have presented the normalized transverse momentum distributions of (a) the hardest jet, (b) the second hardest jet, (c) the hardest lepton and (d) the second hardest lepton. Fig. 3 clearly suggests that mUED model will give rise to very soft leptons and jets at the LHC. This is a consequence of nearly degenerate mUED mass spectrum. As we increase the value of  $R^{-1}$  or  $\Lambda$ , the mass splitting between different  $n = 1$  particles increases. Therefore, we will have relatively harder leptons and jets for large value of  $R^{-1}$  or  $\Lambda$ . The  $p_T$  distribution of leptons show that hardest lepton  $p_T$  does not exceed 60 GeV and we can use a upper cut of 50 GeV on the hardest lepton's transverse momentum to reject Standard Model backgrounds.

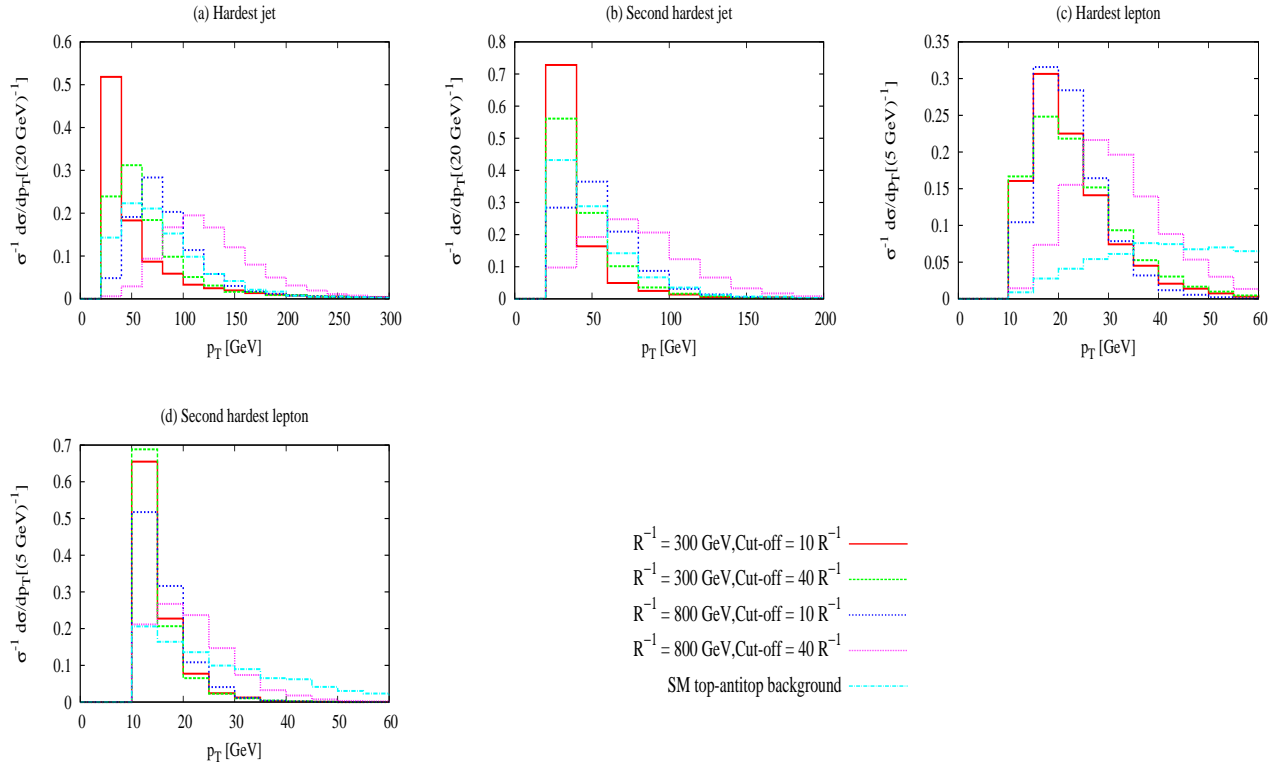


Figure 3: Normalized transverse momentum distributions of the events: (a) the hardest jet, (b) the second hardest jet, (c) the hardest lepton and (d) the second hardest lepton. Each panel shows distributions for four signal points:  $(R^{-1}, \Lambda R) \equiv (300, 10), (300, 40), (800, 10)$  and  $(800, 40)$  GeV and SM  $t\bar{t}$  background.

In the Fig. 4, we have presented the jet multiplicity distribution of signal events. Since we have considered only QCD production channels (namely,  $g_1 g_1$ ,  $g_1 Q_1$ , and  $Q_1 Q_1$ ), all the events are

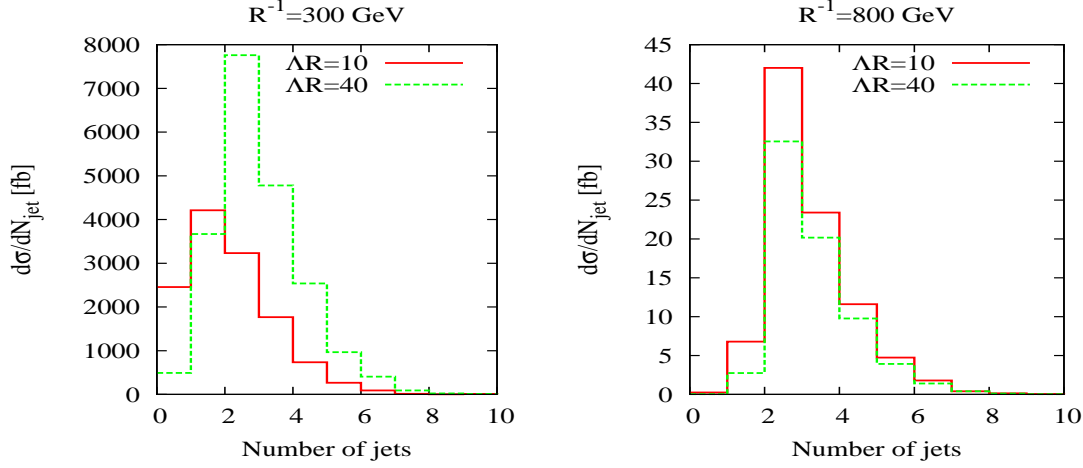


Figure 4: Jet multiplicity distributions for four different signal points. Left panel:  $(R^{-1}, \Delta R) \equiv (300, 10), (300, 40)$  GeV and right panel:  $(R^{-1}, \Delta R) \equiv (800, 10), (800, 40)$  GeV.

accompanied by one or more jets. In fact, more than 79 (96)% of the multilepton events for  $R^{-1} = 300$  (800) GeV and  $\Delta R = 40$  are accompanied by two or more jets. We can exploit this feature of the signal to reduce the contributions from the SM background process (like Single  $W$ ,  $Z$ -boson,  $WW$ ,  $ZZ$ ,  $WZ$  etc. productions) which may have high lepton multiplicity but low jet multiplicity.

In the Fig. 5, we present the normalized  $\frac{\cancel{E}_T}{M_{eff}}$  distributions for four different signal points. A lower bound on the  $\frac{\cancel{E}_T}{M_{eff}}$  could be very efficient to reduce background contributions where  $\cancel{E}_T$  arises from the mis-measurement of visible momenta.

As already explained, the Standard Model background processes most relevant to mUED searches in multilepton mode are  $t\bar{t}$ , single top,  $W + jets$ ,  $Z + jets$  and diboson production. We use PYTHIA to generate signal events and for SM backgrounds ALPGEN [31] and CALCHEP [32] is used. The parton level unweighted events from ALPGEN or CalCHEP has been interfaced with PYTHIA. We use the CTEQ5M parton distribution function in our analysis. The list of the SM background process considered and their cross sections are presented in Table 1. We have used inbuilt initial and final state radiations (ISR/FSR), fragmentation and hadronization routines in the PYTHIA code and we do not consider the effect of multiple interactions.

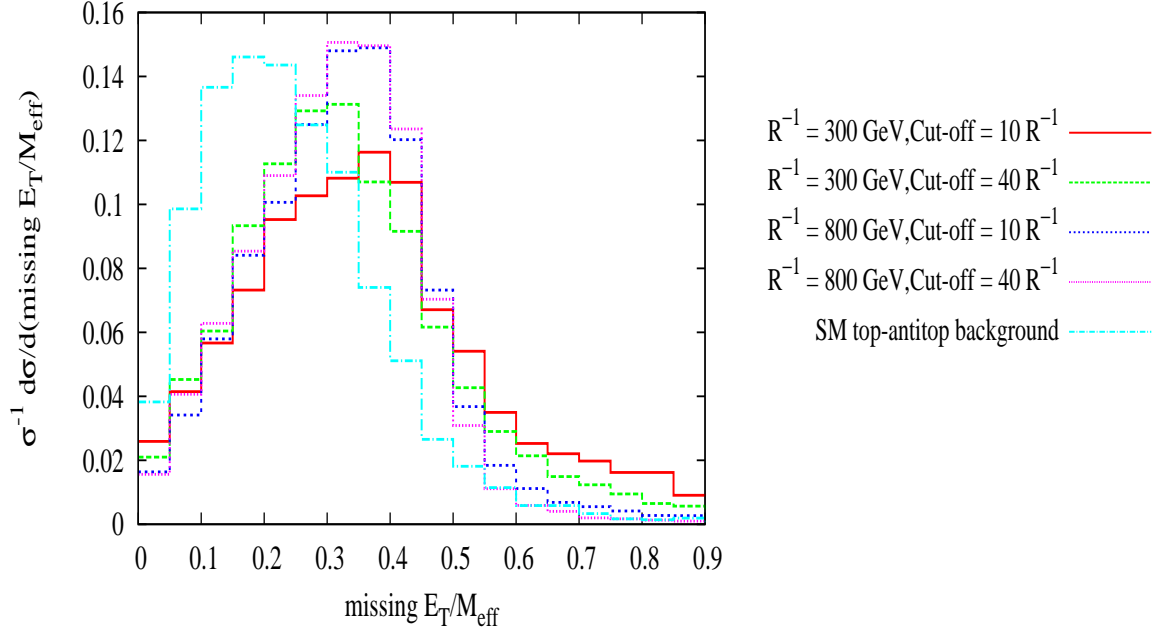


Figure 5: Normalized  $\frac{E_T}{M_{\text{eff}}}$  distributions for four different signal points and SM  $t\bar{t}$  background.

### III.3 Event Selection

After discussing about the signal and background characteristics, we are now equipped enough to introduce a set event selection criteria which will enhance the signal to background ratio. We have applied channel independent as well as channel dependent cuts. We have used b tagging with efficiency  $\epsilon_b = 0.5$  to minimize SM top quark backgrounds. The event selection criteria for different signal topologies under consideration are summarized in the following.

#### III.3.1 Same-sign di-lepton (SSD) events

- We demand exactly one pair of leptons with same charge and  $p_T > 10 \text{ GeV}$ . We reject events with a third lepton with  $p_T > 10 \text{ GeV}$ .
- As discussed in the previous section, the softness of the signal leptons can also be utilized to enhance signal to background ratio. We demand  $p_T^{l_1} < 50 \text{ GeV}$  and  $p_T^{l_2} < 30 \text{ GeV}$  where  $l_1$  and  $l_2$  are the hardest and second hardest lepton respectively.
- We require at least two jets with  $p_T > 40 \text{ GeV}$ . This cut is very efficient in reducing the contribution from SM background which may have high lepton multiplicity but low jet multiplicity.

Process	Generator	Cross section in [pb] $\sqrt{s} = 7 \text{ TeV}$
$t\bar{t}$ : $t\bar{t} + 0, 1 \text{ and } 2 \text{ jets}$	PYTHIA+ALPGEN	113.01
$WW$ : $W^\pm(\rightarrow l\nu) + W^\pm(\rightarrow l\nu) + 0, 1 \text{ and } 2 \text{ jets}$	PYTHIA+ALPGEN	4.23
$ZZ$ : $Z(\rightarrow all) + Z(\rightarrow all) + 0, 1 \text{ and } 2 \text{ jets}$	PYTHIA+ALPGEN	6.75
$WZ$ : $W^\pm(\rightarrow all) + Z(\rightarrow all) + 0, 1 \text{ and } 2 \text{ jets}$	PYTHIA+ALPGEN	15.09
$W + b\bar{b}$ : $W^\pm(\rightarrow all) + b\bar{b}$	PYTHIA+ALPGEN	3.22
$W + t\bar{t}$ : $W^\pm(\rightarrow all) + t\bar{t}$	PYTHIA+ALPGEN	$1.39 \times 10^{-1}$
$Z + b\bar{b}$ : $Z(\rightarrow l\bar{l}) + b\bar{b}$	PYTHIA+ALPGEN	$1.6 \times 10^{-1}$
$Z + t\bar{t}$ : $Z(\rightarrow l\bar{l}) + t\bar{t}$	PYTHIA+ALPGEN	$4.37 \times 10^{-3}$
$W/Z/\gamma$ :	PYTHIA	$4.23 \times 10^5$
$W+\text{jets}$ : $W^\pm(\rightarrow l\nu) + 1 \text{ jet}$	PYTHIA+ALPGEN	$1.00 \times 10^3$
$Z+\text{jets}$ : $Z(\rightarrow l\bar{l}) + 1 \text{ jet}$	PYTHIA+ALPGEN	30.9
$ttt\bar{t}$	PYTHIA+CALcHEP	less than 0.001
$b\bar{b}b\bar{b}$	PYTHIA+CALcHEP	14
$t\bar{t}b\bar{b}$	PYTHIA+CALcHEP	0.14

Table 1: List of Standard Model backgrounds used in our analysis. The cross sections are evaluated with  $\sqrt{s}=7 \text{ TeV}$ , using PYTHIA,ALPGEN and CALcHEP.

- Since the SM events are more likely to have lower  $\cancel{E}_T$ , a higher bound on the  $\cancel{E}_T$  would be very effective against QCD di-jet and  $Z+\text{jets}$  events. However, as discussed earlier, due to the close degeneracy of the mUED mass spectrum, we will not have large  $\cancel{E}_T$  for signal events. Therefore, we demand  $\cancel{E}_T$  to be greater than 50 GeV in all events.
- We require missing  $E_T > f \times M_{eff}$  where  $f = 0.2$ .
- As mentioned earlier, the most dominant SM background process is the  $t\bar{t}$  production followed by the semi-leptonic decay of one b-quark, leptonic decay of one  $W$ -boson and hadronic decay of the other  $W$ -boson.  $t\bar{t}$  contribution can be suppressed by rejecting events with tagged b jets. Therefore, we use b jet veto to minimize the SM top backgrounds.

### III.3.2 Opposite-sign di-lepton (OSD) events

- We require the presence of exactly two leptons with opposite charge and  $p_T > 10 \text{ GeV}$ .
- We impose an upper bound of 50 and 30 GeV on the transverse momentum of the hardest and second hardest lepton respectively.
- We require the missing  $E_T$  to be larger than 50 GeV.
- At least 2 jets with  $p_T > 40 \text{ GeV}$ .

- Missing  $E_T > f \times M_{eff}$  where  $f = 0.2$ .
- We also apply b jet veto to minimize SM top backgrounds.
- We vetoed events exhibiting the same flavour opposite charge lepton pair with an invariant mass smaller than 10 GeV and also invariant mass between 80 to 100 GeV. This cut removes both Z boson and QED contribution.

### III.3.3 Tri-lepton events

- We require the presence of exactly three isolated leptons with  $p_T$  greater than 10 GeV.
- We demand  $p_T^{l_1} < 50$  GeV and  $p_T^{l_2} < 30$  GeV.
- Missing transverse energy  $\cancel{E}_T > 50$  GeV.
- We require atleast 2 jets with  $p_T > 40$  GeV.
- The ratio of missing  $E_T$  and effective mass must be greater than 0.2.
- We put the same cut on the invariant mass on the opposite sign same flavour (ossf) leptons as described above, i.e.,  $|M_{ossf} - M_Z| > 10$  GeV, and  $M_{ossf} > 10$  GeV.
- We also apply b jet veto.

### III.3.4 Four-lepton events

- We require 4 leptons with  $p_T$  greater than 10 GeV. We also require the hardest and second hardest lepton transverse momentum to be less than 50 and 30 GeV respectively.
- Missing  $E_T > 50$  GeV.
- Atleast 2 jets with  $p_T > 40$  GeV.
- We also apply the same invariant mass cut on the opposite sign same flavour leptons and b jet veto as described above.

## III.4 Discovery reach

In this section, we will concentrate on the discovery potential of mUED model at the LHC with centre of mass energy 7 TeV where the maximum integrated luminosity is likely to be of the order of 1 to 2  $fb^{-1}$ . The masses of the KK particles scale linearly with  $R^{-1}$  and hence, total KK cross section decreases with it. We choose  $R^{-1}$  as one of the scan parameter. We have chosen  $\Lambda R$  as the second scan parameter because it determines the splitting between two KK states.

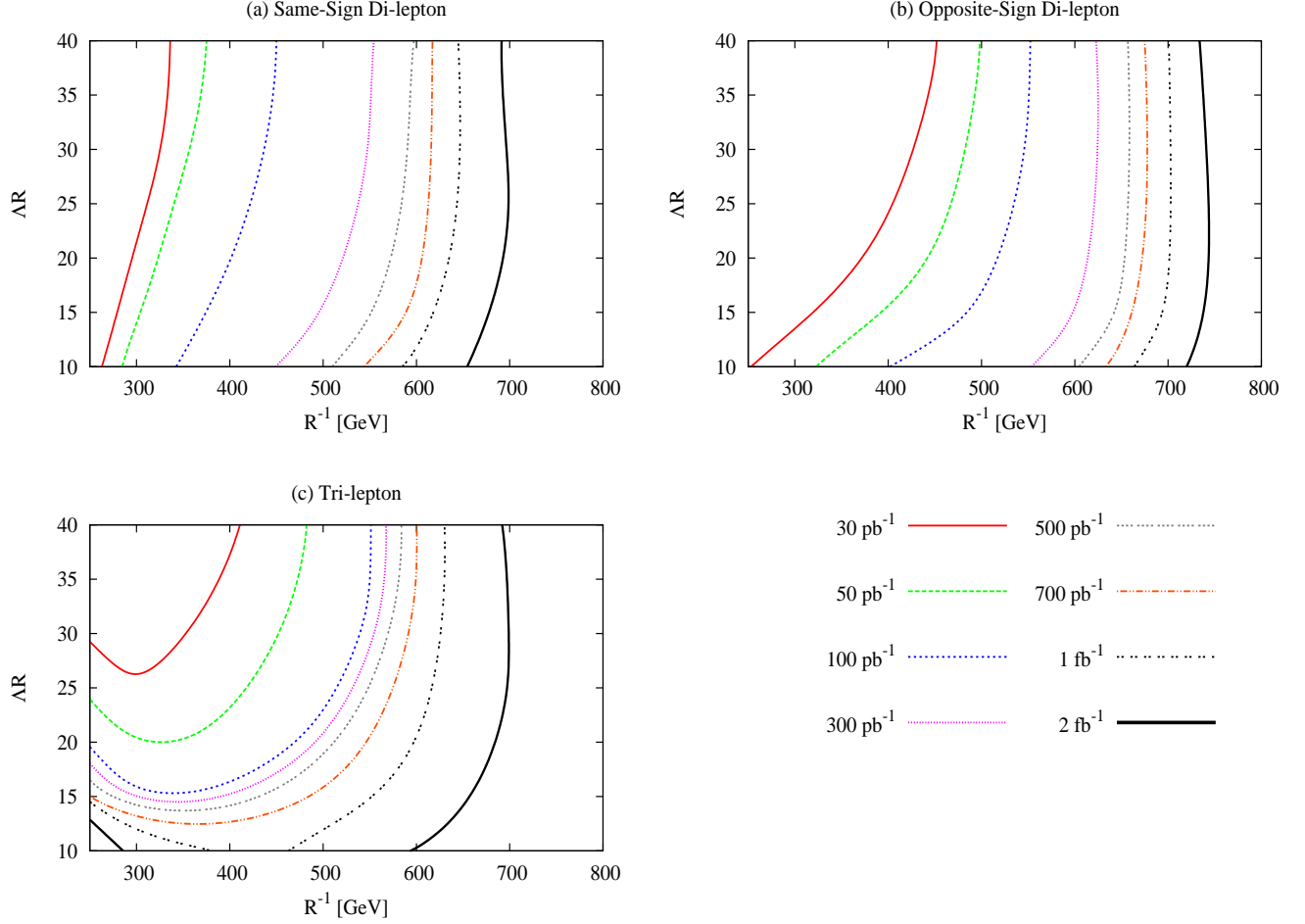


Figure 6: Discovery reach of mUED at the LHC with  $\sqrt{s} = 7$  TeV. (a). Same-sign di-lepton, (b). opposite-sign di-lepton and (c) tri-lepton channel. We have used  $\cancel{E}_T$  to suppress the SM backgrounds. Eight different values of integrated luminosities are assumed. Each line corresponds to  $5\sigma$  contour in the  $R^{-1} - \Lambda R$  plane.

The determination of  $\cancel{E}_T$  crucially depends on the precise knowledge of the detector response. Since fake  $\cancel{E}_T$  grows with the total scalar energy in hadron collider events, the knowledge about the detector performance at  $\sqrt{s} \sim 0.95 - 2.36$  TeV may not be useful. Therefore, at the early stage of LHC with  $\sqrt{s} = 7$  TeV, precise information about the  $\cancel{E}_T$  may not be available. Keeping this in mind, we have divided our analysis into two different categories. For category-1, we assume that there will be precise information about  $\cancel{E}_T$ . We use this information to suppress the SM backgrounds. For category-2, we do not use any information about  $\cancel{E}_T$ .

First, we show the discovery reach in the multileptonic channel using the  $\cancel{E}_T$  i.e., category-1. We define the signal to be observable for a integrated luminosity  $\mathcal{L}$  if,



•

$$\frac{N_S}{\sqrt{N_B + N_S}} \geq 5 \quad \text{for} \quad 0 < N_B \leq 5N_S, \quad (2)$$

where,  $N_{S(B)} = \sigma_{S(B)} \mathcal{L}$ , is the number of signal (background) events for an integrated luminosity  $\mathcal{L}$ .

- For zero number of background event, the signal is observable if there are at least five signal events.
- In order to establish the discovery of a small signal (which could be statistically significant i.e.  $N_S/\sqrt{N_B} \geq 5$ ) on top of a large background, we need to know the background with exquisite precision. However, such precise determination of the SM background is beyond the scope of this present article. Therefore, we impose the requirement  $N_B \leq 5N_S$  to avoid such possibilities.

In Fig. 6, we have presented the mUED discovery potential of the LHC in the multilepton plus  $\cancel{E}_T$  channels namely, (a). same-sign di-lepton, (b). opposite-sign di-lepton and (c) tri-lepton channel. We have assumed eight different values of integrated luminosity ranging over  $30 \text{ pb}^{-1}$  to  $2 \text{ fb}^{-1}$ . Figure shows the  $5\sigma$  discovery contour in the  $R^{-1}$ - $\Lambda R$  plane and the lines refer to the different integrated luminosities.

- Fig. 6 clearly suggests that for low integrated luminosity OSD and tri-lepton channels are most promising. As for example, with  $100 \text{ pb}^{-1}$  integrated luminosity, one can probe mUED parameter space upto  $R^{-1} = 550 \text{ GeV}$  for  $\Lambda R = 30$  in the OSD or tri-lepton channel. Whereas, the corresponding discovery reach in SSD channel is  $R^{-1} = 440 \text{ GeV}$ .
- Fig. 6 shows that discovery potential in these channels strongly depend on the  $\Lambda R$  of the model for low value of  $R^{-1}$  and it is almost independent of  $\Lambda R$  in case of high value of  $R^{-1}$ . It is also clear from the Fig. 6 that probing lower values of the cut-off scale ( $\Lambda$ ) will be difficult i.e. we require higher integrated luminosity to probe low  $\Lambda R$  region. This is a consequence of the fact that lower value cut-off scale will corresponds to more degenerate mUED mass spectrum. If the mass-splitting between different  $n = 1$  KK states are small, the final state leptons and jets (arising from the cascade decay of  $n = 1$  quarks and gluons) will be very soft and fall out side of the detector acceptance quite often. Therefore, for small  $\Lambda R$ , the signal cross-section decreases and we require higher integrated luminosity to probe the region. This feature can be observed in all the three channels, however, most prominent in the tri-lepton channel. Fig. 6c shows that in the tri-lepton channel, one can not probe  $\Lambda R < 20$  region with  $50 \text{ pb}^{-1}$  integrated luminosity. Since the mass splitting increases with in increasing values of  $R^{-1}$ , the sensitivity of  $\Lambda R$  decreases for higher values of  $R^{-1}$ .
- For high integrated luminosity, OSD is the most promising channel and it can probe  $R^{-1} \sim 750$  (700)  $\text{GeV}$  at an integrated luminosity of 2 (1)  $\text{fb}^{-1}$ . This reach is almost independent of the  $\Lambda R$ . The SSD and tri-lepton channels have less background, but the

signal cross sections are also small. The OSD channel, background being an order of magnitude larger, is on the other hand more useful. Hence, the OSD channel results may actually be the most important for the early searches.

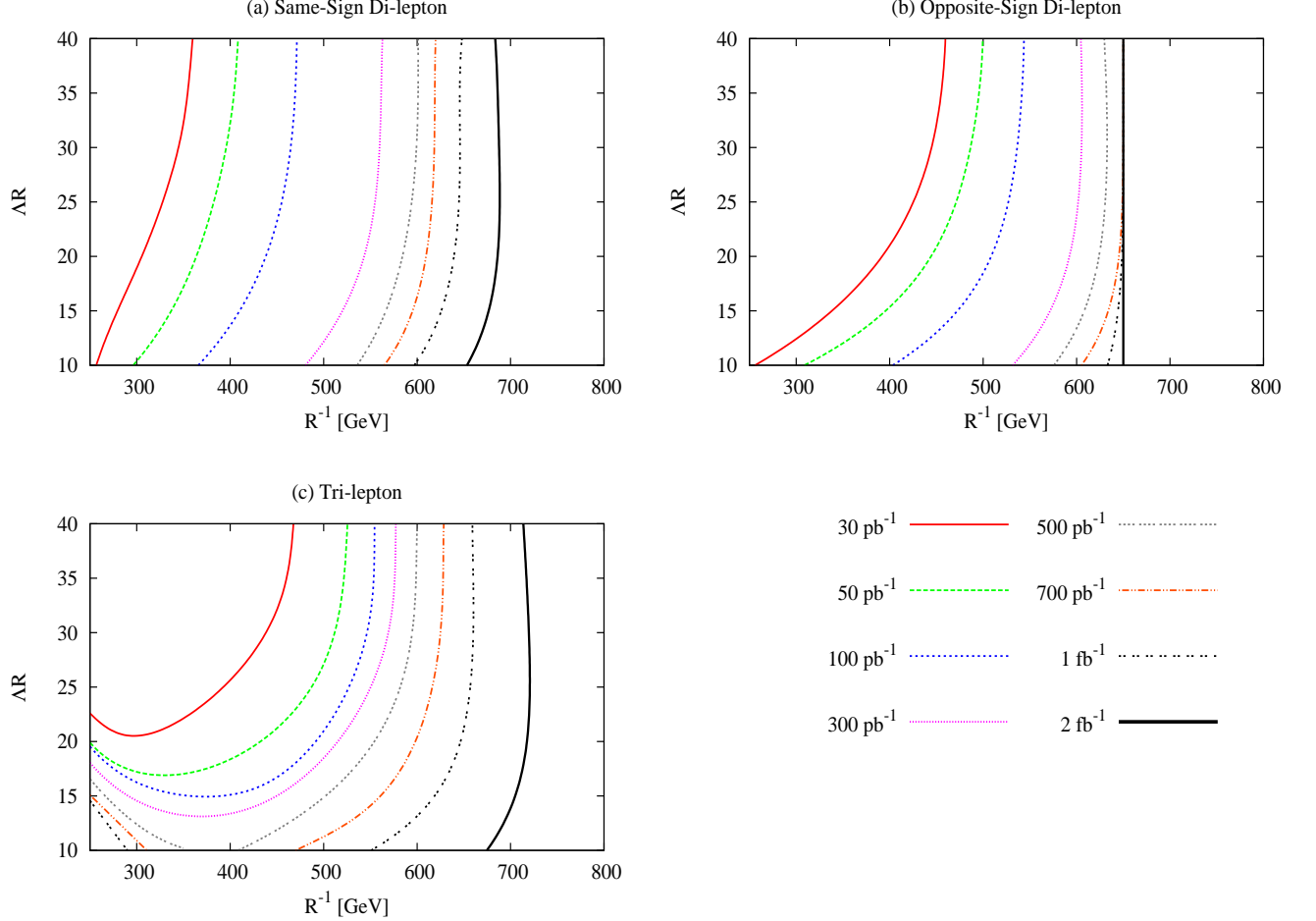


Figure 7: Discovery reach of mUED at the LHC with  $\sqrt{s} = 7$  TeV. (a). Same-sign di-lepton, (b). opposite-sign di-lepton and (c) tri-lepton channel. We do not use any information about the  $\cancel{E}_T$ . Eight different values of integrated luminosities are assumed. Each line corresponds to  $5\sigma$  contour in the  $R^{-1} - \Lambda R$  plane.

As stated earlier, the understanding of the nature of the  $\cancel{E}_T$  will be crucial in the early search for new physics at the LHC. At the early stage of LHC, estimation and the rejection of the background from physics processes with no real intrinsic transverse missing energy is more challenging because the measured  $\cancel{E}_T$  would not reflect the one originating from the non-interacting particles. For this reason, we have carried out the same analysis without considering the  $\cancel{E}_T$  cut. In the Fig. 7, we present the discovery reach of mUED model without using  $\cancel{E}_T$ <sup>5</sup>. The  $\cancel{E}_T$  distribution of this model is soft (see Fig. 2) and therefore, it is expected that inclusion

<sup>5</sup>In this part of our analysis, we do not use  $\cancel{E}_T > 50$  GeV and  $\cancel{E}_T > 0.2 \times M_{eff}$  cuts.

of  $\cancel{E}_T$  can not change the reach significantly. This feature is in contradiction with most of the supersymmetric models. In a recent study [28], it was shown in the context of minimal supergravity model that use of  $\cancel{E}_T$  cut will enhance the LHC reach significantly. However, in our case, if we do not use the  $\cancel{E}_T$  cuts, the reach of  $R^{-1}$  slightly reduced except in the tri-lepton channel (see Fig. 7).

Here also, for low integrated luminosity, OSD and tri-lepton channels are most promising. However, for high integrated luminosity, tri-lepton is the most promising channel because of the low SM background. As for example, with  $2 \text{ fb}^{-1}$  integrated luminosity, mUED parameter space can be probed upto  $R^{-1} = 714$  (675) GeV for  $\Lambda R = 40$  (10) in the tri-lepton channel. However, in the SSD and OSD channel the discovery reach is  $R^{-1} = 683$  (653) and 650 (650) GeV respectively for  $\Lambda R = 40$  (10). As we increase  $R^{-1}$ , the total pair production cross-section of  $Q_1$  and  $g_1$  decreases (see Fig. 1) and hence, the signal cross-section decreases. In defining the observability of the signal, we have demanded that  $\sigma_S > \sigma_B/5$ . The SM background for the OSD channel is quite large. Therefore, we can not probe  $R^{-1}$  beyond 650 GeV in the OSD channel by increasing integrated luminosity.

Here we do not show the discovery reach in the 4 lepton channel separately because the 4 lepton cross section is much smaller than other three processes considered here. As for example, we obtain 4-lepton cross-section (with the  $\cancel{E}_T$  cuts) of 3.21 (1.69) fb for  $R^{-1} = 400$  (600) GeV and  $\Lambda R = 20$ . Therefore, we have not found atleast 5 events in most of the parameter space points. It is possible to combine the significance of these channels but no such attempt has made in our paper.

## IV Conclusion

In this paper we have investigated the early discovery signals of minimal UED model at the Large Hadron Collider with center of mass energy 7 TeV and integrated luminosity  $1 \text{ fb}^{-1}$ . We have considered signals with two or more leptons in the final state and we have calculated the discovery reach in each of the final states. The results of our work indicates that LHC can discover the signals of mUED if  $R^{-1}$  is less than 700 GeV. The opposite sign di-lepton channel is the most promising one. We have seen that the inclusion of missing energy does not change the discovery limit drastically. This is due to the fact that the  $\cancel{E}_T$  distribution of mUED model has the similar shape as the SM backgrounds. It should be stressed that our cuts are very simple and reach may be improved by imposing more specific cuts. In summary, we can say that early LHC data has substantial reach within the mUED parameter space.

**Acknowledgement:** The authors would like to thank the organizers of WHEPP-XI (Ahmedabad, 2010) where some of this work was done. BB thanks Sreerup Raychaudhuri and Anirban Kundu for many useful discussions. KG acknowledges the support available from the Department of Atomic Energy, Government of India, for the Regional Centre for Accelerator-based Particle Physics (RECAPP), Harish-Chandra Research Institute. Computational work for this study was partially carried out at the cluster computing facility in the Harish-Chandra Research

## References

- [1] T. Appelquist, H. C. Cheng and B. A. Dobrescu, Phys. Rev. D **64**, 035002 (2001) [arXiv:hep-ph/0012100].
- [2] H. C. Cheng, K. T. Matchev and M. Schmaltz, Phys. Rev. D **66**, 036005 (2002) [arXiv:hep-ph/0204342].
- [3] H. C. Cheng, K. T. Matchev and M. Schmaltz, Phys. Rev. D **66**, 056006 (2002) [arXiv:hep-ph/0205314].
- [4] B. A. Dobrescu and E. Ponton, JHEP **0403**, 071 (2004) [arXiv:hep-th/0401032]; G. Burdman, B. A. Dobrescu and E. Ponton, JHEP **0602**, 033 (2006) [arXiv:hep-ph/0506334].
- [5] T. Appelquist, B. A. Dobrescu, E. Ponton and H. U. Yee, Phys. Rev. Lett. **87**, 181802 (2001) [arXiv:hep-ph/0107056].
- [6] B. A. Dobrescu and E. Poppitz, Phys. Rev. Lett. **87**, 031801 (2001) [arXiv:hep-ph/0102010].
- [7] G. Burdman, B. A. Dobrescu and E. Ponton, Phys. Rev. D **74**, 075008 (2006) [arXiv:hep-ph/0601186]; B. A. Dobrescu, K. Kong and R. Mahbubani, JHEP **0707**, 006 (2007) [arXiv:hep-ph/0703231]; A. Freitas and K. Kong, JHEP **0802**, 068 (2008) [arXiv:0711.4124 [hep-ph]]; K. Ghosh and A. Datta, Nucl. Phys. B **800**, 109 (2008) [arXiv:0801.0943 [hep-ph]]; K. Ghosh and A. Datta, Phys. Lett. B **665**, 369 (2008) [arXiv:0802.2162 [hep-ph]]; K. Ghosh, JHEP **0904**, 049 (2009) [arXiv:0809.1827 [hep-ph]].
- [8] A. Freitas and U. Haisch, Phys. Rev. D **77**, 093008 (2008) [arXiv:0801.4346 [hep-ph]]; U. Haisch, arXiv:0805.2141 [hep-ph].
- [9] B. A. Dobrescu, D. Hooper, K. Kong and R. Mahbubani, JCAP **0710**, 012 (2007) [arXiv:0706.3409 [hep-ph]].
- [10] S. Dimopoulos and H. Georgi, Nucl. Phys. **B 193** (1981) 150; N. Sakai, Z. Physik **C 11** (1981) 153; H. Baer and X. Tata, *Weak Scale Supersymmetry: From Superfields to Scattering Events*, (Cambridge University Press, 2006); M. Drees, R. Godbole and P. Roy, *Theory and Phenomenology of Sparticles*, (World Scientific, 2004); P. Binetruy, *Supersymmetry* (Oxford University Press, 2006); S. P. Martin, hep-ph/9709356; A. Chamseddine, R. Arnowitt and P. Nath, Phys. Rev. Lett. **49**, 970 (1982); R. Barbieri, S. Ferrara and C. Savoy, Phys. Lett B **119**, 343 (1982); N. Ohta, Prog. Theor. Phys. **70**, 542 (1983); L. Hall, J. Lykken and S. Weinberg, Phys. Rev. D **27**, 2359 (1983).
- [11] H. Georgi, A. K. Grant and G. Hailu, Phys. Lett. B **506**, 207 (2001) [arXiv:hep-ph/0012379].

- [12] G. von Gersdorff, N. Irges and M. Quiros, Nucl. Phys. B **635**, 127 (2002) [arXiv:hep-th/0204223]; L. Da Rold, Phys. Rev. D **69**, 105015 (2004) [arXiv:hep-th/0311063]; E. Alvarez and A. F. Faedo, JHEP **0605**, 046 (2006) [arXiv:hep-th/0602150].
- [13] G. Servant and T. M. P. Tait, Nucl. Phys. B **650**, 391 (2003) [arXiv:hep-ph/0206071]; H. C. Cheng, J. L. Feng and K. T. Matchev, Phys. Rev. Lett. **89**, 211301 (2002) [arXiv:hep-ph/0207125]; M. Kakizaki, S. Matsumoto, Y. Sato and M. Senami, Phys. Rev. D **71**, 123522 (2005) [arXiv:hep-ph/0502059]; M. Kakizaki, S. Matsumoto, Y. Sato and M. Senami, Nucl. Phys. B **735**, 84 (2006) [arXiv:hep-ph/0508283]; F. Burnell and G. D. Kribs, Phys. Rev. D **73**, 015001 (2006) [arXiv:hep-ph/0509118]; K. Kong and K. T. Matchev, JHEP **0601**, 038 (2006) [arXiv:hep-ph/0509119]; M. Kakizaki, S. Matsumoto and M. Senami, Phys. Rev. D **74**, 023504 (2006) [arXiv:hep-ph/0605280]; D. Hooper and S. Profumo, Phys. Rept. **453**, 29 (2007) [arXiv:hep-ph/0701197].
- [14] P. Nath and M. Yamaguchi, Phys. Rev. D **60** (1999) 116006 [arXiv:hep-ph/9903298]; K. Agashe, N. G. Deshpande and G. H. Wu, Phys. Lett. B **511**, 85 (2001) [arXiv:hep-ph/0103235].
- [15] D. Chakraverty, K. Huitu and A. Kundu, Phys. Lett. B **558** (2003) 173 [arXiv:hep-ph/0212047].
- [16] A.J. Buras, M. Spranger and A. Weiler, Nucl. Phys. B **660** (2003) 225 [arXiv:hep-ph/0212143]; A.J. Buras, A. Poschenrieder, M. Spranger and A. Weiler, Nucl. Phys. B **678** (2004) 455 [arXiv:hep-ph/0306158].
- [17] K. Agashe, N.G. Deshpande and G.H. Wu, Phys. Lett. B **514** (2001) 309 [arXiv:hep-ph/0105084].
- [18] J.F. Oliver, J. Papavassiliou and A. Santamaria, Phys. Rev. D **67** (2003) 056002 [arXiv:hep-ph/0212391].
- [19] T. Appelquist and H. U. Yee, Phys. Rev. D **67** (2003) 055002 [arXiv:hep-ph/0211023].
- [20] T. G. Rizzo and J.D. Wells, Phys. Rev. D **61** (2000) 016007 [arXiv:hep-ph/9906234]; A. Strumia, Phys. Lett. B **466** (1999) 107 [arXiv:hep-ph/9906266]; C.D. Carone, Phys. Rev. D **61** (2000) 015008 [arXiv:hep-ph/9907362]; I. Gogoladze and C. Macesanu, Phys. Rev. D **74**, 093012 (2006) [arXiv:hep-ph/0605207].
- [21] B. Abbott *et al.* [D0 Collaboration], Phys. Rev. Lett. **83**, 4937 (1999) [arXiv:hep-ex/9902013].
- [22] C. Lin, “A Search for universal extra dimensions in the multi-lepton channel from  $p\bar{p}$  collisions at  $\sqrt{s} = 1.8$  TeV,” UMI-31-94684.
- [23] U. Haisch and A. Weiler, Phys. Rev. D **76** (2007) 034014 [arXiv:hep-ph/0703064].

- [24] K. Dienes, E. Dudas, and T. Gherghetta; Nucl. Phys. B **537** (1999) 47 [arXiv:hep-ph/9806292]; K. R. Dienes, E. Dudas and T. Gherghetta, Phys. Lett. B **436** (1998) 55 [arXiv:hep-ph/9803466].
- [25] G. Bhattacharyya, A. Datta, S. K. Majee and A. Raychaudhuri, Nucl. Phys. B **760**, 117 (2007) [arXiv:hep-ph/0608208].
- [26] T. G. Rizzo, Phys. Rev. D **64**, 095010 (2001) [arXiv:hep-ph/0106336]; C. Macesanu, C. D. McMullen and S. Nandi, Phys. Rev. D **66**, 015009 (2002) [arXiv:hep-ph/0201300]; H. C. Cheng, K. T. Matchev and M. Schmaltz, Phys. Rev. D **66**, 056006 (2002) [arXiv:hep-ph/0205314]; H. C. Cheng, Int. J. Mod. Phys. A **18**, 2779 (2003) [arXiv:hep-ph/0206035]; C. Macesanu, C. D. McMullen and S. Nandi, Phys. Lett. B **546**, 253 (2002) [arXiv:hep-ph/0207269]; A. Muck, A. Pilaftsis and R. Ruckl, Nucl. Phys. B **687**, 55 (2004) [arXiv:hep-ph/0312186]; C. Macesanu, S. Nandi and M. Rujoiu, Phys. Rev. D **71**, 036003 (2005) [arXiv:hep-ph/0407253]; G. Bhattacharyya, et al, Phys. Lett. B **628**, 141 (2005) [arXiv:hep-ph/0502031]; M. Battaglia, A. Datta, A. De Roeck, K. Kong and K. T. Matchev, JHEP **0507**, 033 (2005) [arXiv:hep-ph/0502041]; M. Battaglia, A. K. Datta, A. De Roeck, K. Kong and K. T. Matchev, *In the Proceedings of 2005 International Linear Collider Workshop (LCWS 2005), Stanford, California, 18-22 Mar 2005, pp 0302* [arXiv:hep-ph/0507284]; A. K. Datta, K. Kong and K. T. Matchev, *In the Proceedings of 2005 International Linear Collider Workshop (LCWS 2005), Stanford, California, 18-22 Mar 2005, pp 0215* [arXiv:hep-ph/0508161]; B. Bhattacharjee and A. Kundu, Phys. Lett. B **627**, 137 (2005) [arXiv:hep-ph/0508170]; A. Datta, K. Kong and K. T. Matchev, Phys. Rev. D **72**, 096006 (2005) [Erratum-ibid. D **72**, 119901 (2005)] [arXiv:hep-ph/0509246]; A. Datta and S. K. Rai, Int. J. Mod. Phys. A **23**, 519 (2008) [arXiv:hep-ph/0509277]; A. Datta, G. L. Kane and M. Toharia, [arXiv:hep-ph/0510204]; S. K. Rai, Int. J. Mod. Phys. A **23**, 823 (2008) [arXiv:hep-ph/0510339]; A. J. Barr, JHEP **0602**, 042 (2006) [arXiv:hep-ph/0511115]; B. Bhattacharjee and A. Kundu, J. Phys. G **32**, 2123 (2006) [arXiv:hep-ph/0605118]; B. Bhattacharjee and A. Kundu, Phys. Lett. B **653**, 300 (2007) [arXiv:0704.3340 [hep-ph]]; G. H. Brooijmans *et al.*, [arXiv:0802.3715 [hep-ph]]; B. Bhattacharjee *et al.*, Phys. Rev. D **78**, 115005 (2008) [arXiv:0805.3619 [hep-ph]]; B. Bhattacharjee, Phys. Rev. D **79**, 016006 (2009) [arXiv:0810.4441 [hep-ph]]; M. ElKacimi, D. Goujdami, H. Przysieznik and P. Z. Skands, Comput. Phys. Commun. **181**, 122 (2010) [arXiv:0901.4087 [hep-ph]]; G. Bhattacharyya, et al, Nucl. Phys. B **821**, 48 (2009) [arXiv:0904.0937 [hep-ph]]; P. Bandyopadhyay, B. Bhattacharjee and A. Datta, JHEP **1003**, 048 (2010) [arXiv:0909.3108 [hep-ph]]; D. Choudhury, A. Datta and K. Ghosh, arXiv:0911.4064 [hep-ph]; K. Kong, K. Matchev and G. Servant, arXiv:1001.4801 [hep-ph].
- [27] For a recent work on supersymmetry search, see, for example, J. Edsjo, E. Lundstrom, S. Rydbeck and J. Sjolín, JHEP **1003**, 054 (2010) [arXiv:0910.1106 [hep-ph]]; N. Ozturk [ATLAS Collaboration and CMS Collaboration], arXiv:0910.2964 [hep-ex]; H. Baer, S. Kraml, A. Lessa and S. Sekmen, JHEP **1002**, 055 (2010) [arXiv:0911.4739 [hep-ph]]; M. H. Genest [CMS Collaboration and ATLAS Collaboration], arXiv:0912.4378 [hep-ex]; M. Pioppi [CMS Collaboration], arXiv:0912.1189 [hep-ex]; D. Feldman, G. Kane, R. Lu and

- B. D. Nelson, Phys. Lett. B **687**, 363 (2010) [arXiv:1002.2430 [hep-ph]]; H. Baer, S. de Alwis, K. Givens, S. Rajagopalan and H. Summy, JHEP **1005**, 069 (2010) [arXiv:1002.4633 [hep-ph]]; H. K. Dreiner, M. Kramer, J. M. Lindert and B. O’Leary, JHEP **1004**, 109 (2010) [arXiv:1003.2648 [hep-ph]]; K. Choi, D. Guadagnoli, S. H. Im and C. B. Park, arXiv:1005.0618 [hep-ph]. N. Bhattacharyya, A. Datta and S. Poddar, arXiv:1005.2673 [hep-ph].
- [28] H. Baer, V. Barger, A. Lessa and X. Tata, arXiv:1004.3594 [hep-ph].
- [29] B. Bhattacharjee, A. Kundu, S. K. Rai and S. Raychaudhuri, Phys. Rev. D **81**, 035021 (2010) [arXiv:0910.4082 [hep-ph]].
- [30] T. Sjostrand, S. Mrenna and P. Z. Skands, JHEP **0605**, 026 (2006) [arXiv:hep-ph/0603175].
- [31] M. L. Mangano, M. Moretti, F. Piccinini, R. Pittau and A. D. Polosa, JHEP **0307**, 001 (2003) [arXiv:hep-ph/0206293].
- [32] A. Pukhov, arXiv:hep-ph/0412191.